Pergamon

J. Mech. Phys. Solids, Vol. 44, No. 6, pp. 929–951, 1996

0022–5096/96 $15.00+0.00

PII S0022-5096(96)00012-9

ENERGY-RELEASE RATE AND CRACK KINKING IN ANISOTROPIC BRITTLE SOLIDS

ABBAS AZHDARI and SIA NEMAT-NASSER

Center of Excellence for Advanced Materials, Department of Applied Mechanics and Engineering Sciences, University of California, San Diego, La Jolla, CA 92093-0416, U.S.A.

(*Received* 10 *May* 1995; *in revised form* 5 *December* 1995)

ABSTRACT

The energy-release rate is calculated for the inception of crack kinking in a general anisotropic solid containing a pre-existing crack. First, the stress intensity factors at the tip of an infinitesimally small kink ($K_{\mathrm{I}}^{(k)}$ and $K_{\mathrm{II}}^{(k)}$) and the kink opening displacements (KODs) are numerically calculated by modeling the kink as continuously distributed edge dislocations. The energy-release rate, G^{kink}, is obtained directly by calculating the work required to fully close the kink gap (KOD) and restore the required normal and shear stresses ($\sigma_{\omega\omega}$ and $\sigma_{r\omega}$) that existed before kinking. This energy-release rate, G^{kink}, is compared with that (denoted by G^{Irwin}) obtained by applying the Irwin formula in terms of the stress intensity factors $K_{\mathrm{I}}^{(k)}$ and $K_{\mathrm{II}}^{(k)}$ at the tip of the vanishingly small kink, for various kink angles, material properties, material symmetry orientations, and loadings. It is observed that the two methods yield exactly the same value for the rate of energy released, even though G^{kink} corresponds to *kink nucleation*, whereas G^{Irwin} to *kink extension*. Therefore, Irwin's formula for the energy-release rate is valid for any kink angle, material anisotropy, and loading condition (any combination of modes I and II), provided that the stress intensity factors in the formula are taken equal to those calculated at the tip of a vanishingly small kink, but not those associated with the stress components $\sigma_{\omega\omega}$ and $\sigma_{r\omega}$ prior to kinking. For different loading and material symmetry conditions, the energy-release-rate fracture criterion is compared with different stress-based fracture criteria of the fracture-path prediction. Copyright © 1996 Elsevier Science Ltd

INTRODUCTION

Crack kinking is an important feature of fracturing, especially in brittle materials. It often occurs in response to an antisymmetric crack tip stress field, i.e. an anisotropic stress condition can cause crack kinking. This may be due to the anisotropy in the material properties (e.g. single crystals), the antisymmetry in the applied loads, or the complexity in the overall geometry. Therefore, isotropic as well as anisotropic solids may experience the phenomenon of crack kinking. Different criteria are proposed to predict the kink direction. The maximum-K_{I}, zero-K_{II}, and the maximum-hoop stress fracture criteria are based on the near crack-tip stress field that exists prior to the onset of kinking, whereas the maximum energy-release rate, an energy-based fracture criterion, is based on thermodynamic principles (Nemat-Nasser, 1979) and is a generalization of Griffith's original energy-release-rate criterion (Griffith, 1921, 1924). The objective of the present work is to investigate the kinking from a straight crack, on the basis of the maximum energy-release-rate criterion, in a general (two-dimensional) anisotropic solid.

There are several studies regarding the phenomenon of crack kinking in isotropic solids that employ the maximum energy-release-rate criterion, e.g. Hussain *et al.* (1974), Gupta (1976), Palaniswamy and Knauss (1978), Wu (1978a, b, 1979a, b), and Hayashi and Nemat-Nasser (1981a, b). For small kink angles, Wu (1979a) and Hayashi and Nemat-Nasser (1981a) obtained closed-form expressions for the energy-release rate G. In addition, Hayashi and Nemat-Nasser (1981b) examined the validity of Irwin's formula for crack kinking. Irwin's formula for the energy-release-rate calculation is originally derived for a collinear crack extension. It expresses the energy-release rate as a quadratic function of the modes I and II stress intensity factors at the extended crack tip. Hussain *et al.* (1974) first suggested that Irwin's formula may be used to calculate G at the inception of kinking, provided that the stress intensity factors in the formula are the ones that exist at the tip of the vanishingly small kink. This suggestion was questioned by Wu (1978b), and finally verified by Hayashi and Nemat-Nasser (1981b) to be true for isotropic materials, i.e. Hayashi and Nemat-Nasser (1981b) made it clear that Irwin's formula indeed holds at the inception of kinking for all kink angles, and is not limited to only the collinear crack extension.

The extension of Irwin's formula to the case of anisotropic solids first appeared in Sih *et al.* (1965) for a collinear crack extension. The formula was obtained by calculating the work required to close the collinear infinitesimal crack extension by using the asymptotic stress and displacement components at the crack tip. Other equivalent expressions for G (for collinear crack extension) have also been obtained, e.g. Barnett and Asaro (1972); see also Bilby and Eshelby (1968) for a discussion of the concept of the energy-release rate. Irwin's formula has been used to calculate G at the inception of kinking in anisotropic solids; see Obata *et al.* (1989) and Gao and Chiu (1992). The modification consists of transferring all the parameters in the original formula (from the crack direction) to the kink direction. The main objective of the present work is to investigate the validity of this application.

For an infinitesimally small kink, the stress fields resulting from the kink tip and kink knee are both singular and present, whereas for a collinear crack extension, there is no additional singular stress field as a result of a knee. Moreover, Irwin's formula defines G for an infinitesimal extension of a vanishingly small existing kink, whereas crack kinking requires energy for the kink nucleation. To investigate whether Irwin's formula yields the energy-release rate for the kink nucleation, one must calculate G, starting from a basic definition of the energy-release rate, and then compare the results with those obtained using the Irwin equation.

To this end, consider a central main crack in an infinite, homogeneous, anisotropic, and linearly elastic plane that is loaded uniformly at infinity. The normal and shear stresses ($\sigma_{\omega\omega}$ and $\sigma_{r\omega}$) that are transmitted across a line of orientation ω, emanating from the crack tip, are given in terms of the hoop and shear stress intensity factors, HSIF and SSIF; see Azhdari and Nemat-Nasser (1995). Next, consider an infinitesimally small kink in the direction of ω, and solve this new boundary-value problem by the method that models a kink as a continuous distribution of edge dislocations; Lo (1978). This gives the stress intensity factors at the tip of the vanishingly small kink ($K_{\mathrm{I}}^{(\mathrm{k})}$ and $K_{\mathrm{II}}^{(\mathrm{k})}$), as well as the gap between the two kink surfaces (kink opening displacements, KODs). For a direct calculation of the energy-release rate, evaluate the work required to fully close the gap (KOD) and restore along the kink line the

original stress field before kinking ($\sigma_{\omega\omega}$ and $\sigma_{r\omega}$); denote this energy-release rate by G^{kink}. Alternatively, use $K_{\text{I}}^{(\text{k})}$ and $K_{\text{II}}^{(\text{k})}$ in Irwin's formula to calculate the energy-release rate; denote this indirect calculation of the energy-release rate by G^{Irwin}. Next, investigate the relation between G^{kink} and G^{Irwin}.

Several different conditions, i.e. different kink angles, material properties, material symmetry orientations, and loadings are considered. The energy-release rate is calculated by using both Irwin's (G^{Irwin}) and the direct (G^{kink}) methods. It is observed that the two methods yield exactly the same value for the energy-release rate, even though the HSIF and SSIF may differ from $K_{\text{I}}^{(\text{k})}$ and $K_{\text{II}}^{(\text{k})}$ by more than 100%. Therefore, Irwin's formula for the energy-release rate is valid for any kink angle, material anisotropy, and loading condition (any combination of modes I and II), provided that the stress intensity factors in the formula are taken equal to those calculated at the tip of a vanishingly small kink. It is worth noting that *the equality between G^{Irwin} and G^{kink} stems from the fact that $K_{\text{I}}^{(\text{k})}$ and $K_{\text{II}}^{(\text{k})}$ are independent of the length of the vanishingly small kink*; see Appendix and also Azhdari (1995).

The energy-release rate is used to predict the kink orientation and the results are compared with those predicted by other criteria (i.e. maximum-K_{I} or zero-K_{II} and maximum-hoop stress or, equivalently, maximum-hoop stress intensity factor, maximum-HSIF). It is shown that these other criteria do *not* yield the same results as those obtained by the maximum energy-release-rate criterion. This is in contrast to the isotropic case, where all the fracture criteria lead to fairly similar fracture predictions. Hence, the validity and the relevance of the energy-release rate and other competing fracture criteria must be established through experimental studies.

FORMULATION

Statement of problem

Consider plane deformation (plane strain or plane stress) of an anisotropic, homogeneous, linearly elastic plane which contains a traction-free kinked crack. A fixed rectangular Cartesian coordinate system, (x, y), is used where the x-axis coincides with the main crack and the kink is at an angle ω with respect to the x-axis, as shown in Fig. 1. Two supplementary Cartesian coordinate systems, (x_1, x_2) and (ζ, η), are

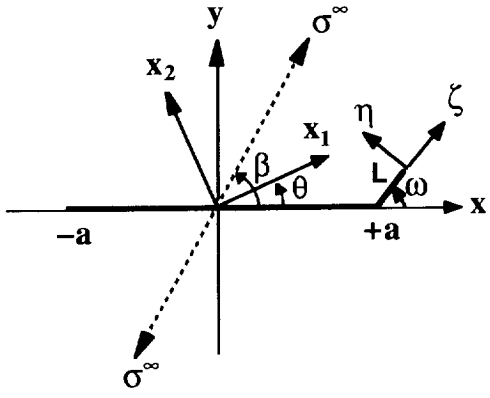

Fig. 1. Geometry, coordinate systems, and loading direction.

also used to indicate the material and the kink-tip coordinate systems, respectively. In what follows, a prime denotes differentiation with respect to the corresponding argument, and an overbar represents the complex conjugate of the corresponding variable. The body is under uniform farfield tractions, σ^∞, acting at an angle β relative to the crack. This applied tension, σ^∞, is equivalent to two tensile stresses and a shear stress, applied at infinity, as follows

$$\sigma^\infty_{xx} = \sigma^\infty \cos^2\beta, \quad \sigma^\infty_{yy} = \sigma^\infty \sin^2\beta, \quad \sigma^\infty_{xy} = \sigma^\infty \sin\beta\cos\beta. \tag{1a–c}$$

Therefore, the farfield loading is non-symmetric unless $\beta = \pm 90^\circ$ (or $\beta = 0^\circ$, which is uninteresting).

Let the body be in the state of plane stress or plane strain. For the plane-stress condition in the x, y-plane, the strain–stress relations are

$$\begin{aligned} \varepsilon_{xx} &= C_{11}\sigma_{xx} + C_{12}\sigma_{yy} + C_{16}\sigma_{xy}, \\ \varepsilon_{yy} &= C_{12}\sigma_{xx} + C_{22}\sigma_{yy} + C_{26}\sigma_{xy}, \\ 2\varepsilon_{xy} &= C_{16}\sigma_{xx} + C_{26}\sigma_{yy} + C_{66}\sigma_{xy}, \end{aligned} \tag{2a–c}$$

where $C_{ij} = C_{ji}$; $i, j = 1, 2, 6$, are the relevant elements of the compliance matrix of the material in the x, y-coordinate system. Plane-strain solutions can be obtained by simply changing the compliance matrix from C_{ij} to $C_{ij} - (C_{i3}C_{j3})/C_{33}$.

It has been shown that (e.g. Savin, 1961; Lekhnitskii, 1963) the problems of two-dimensional anisotropic elasticity can be conveniently formulated in terms of two independent analytic functions, $\phi(z_1)$ and $\psi(z_2)$, where $z_i = x + \mu_i y$, with the two complex numbers μ_1 and μ_2 being the roots of the characteristic equation

$$C_{11}\mu^4 - 2C_{16}\mu^3 + (2C_{12} + C_{66})\mu^2 - 2C_{26}\mu + C_{22} = 0. \tag{3}$$

Owing to the positive-definiteness of the elastic energy, the characteristic equation has either complex or purely imaginary roots that are pairwise each other's complex conjugate. We choose μ_1 and μ_2 such that their imaginary parts are positive. Note that the isotropic case may be regarded as the limiting case for which $\mu_1 = \mu_2 = \mathrm{i} = \sqrt{-1}$. For more details in the use of the complex variable method to solve a two-dimensional crack-kinking problem in anisotropic elasticity, see Obata *et al.* (1989).

Hoop and shear stresses at the tip of the main crack before kinking

In order to calculate the energy that is released as a result of the occurrence of kinking, one needs to calculate the hoop and shear stresses at the tip of the main crack before kinking. In particular, we are interested in the points in the vicinity of the main crack tip, i.e. the asymptotic forms of the hoop stress $\sigma_{\omega\omega}$ and shear stress $\sigma_{r\omega}$ with respect to the distance from the crack tip; see Fig. 2. This is given in detail by Azhdari and Nemat-Nasser (1995). In brief, however, the procedure is given next.

Define the following two stress intensity factors (hoop and shear stress intensity factors, HSIF and SSIF) associated with the hoop and shear stresses at an arbitrary angle ω

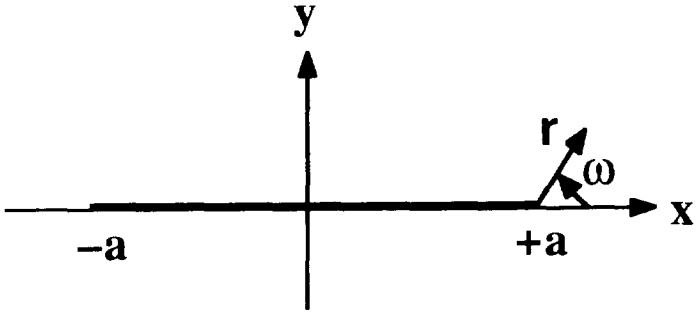

Fig. 2. Polar coordinates at the main crack tip.

$$K_{\omega\omega} \equiv \lim_{r\to 0}(\sqrt{2\pi r}\,\sigma_{\omega\omega}), \quad K_{r\omega} \equiv \lim_{r\to 0}(\sqrt{2\pi r}\,\sigma_{r\omega}), \tag{4a,b}$$

where r is the distance from the crack tip. Using this definition, one can show that HSIF and SSIF become

$$K_{\omega\omega} = K_{11}K_{\mathrm{I}}^{\infty} + K_{12}K_{\mathrm{II}}^{\infty}, \quad K_{r\omega} = K_{21}K_{\mathrm{I}}^{\infty} + K_{22}K_{\mathrm{II}}^{\infty} \tag{5a,b}$$

where

$$K_{\mathrm{I}}^{\infty} = K_{\omega\omega}(\omega = 0) = \sigma_{yy}^{\infty}\sqrt{\pi a} \quad \text{and} \quad K_{\mathrm{II}}^{\infty} = K_{r\omega}(\omega = 0) = \sigma_{xy}^{\infty}\sqrt{\pi a} \tag{6a,b}$$

are the so-called the *apparent stress intensity factors*, and K_{ij}s are defined by

$$K_{11} = \mathrm{Re}\left[\frac{1}{\mu_2-\mu_1}\{\mu_2(c+\mu_1 s)^{3/2} - \mu_1(c+\mu_2 s)^{3/2}\}\right],$$

$$K_{12} = \mathrm{Re}\left[\frac{1}{\mu_2-\mu_1}\{(c+\mu_1 s)^{3/2} - (c+\mu_2 s)^{3/2}\}\right],$$

$$K_{21} = \mathrm{Re}\left[\frac{1}{\mu_2-\mu_1}\{\mu_2(c+\mu_1 s)^{1/2}(s-\mu_1 c) - \mu_1(c+\mu_2 s)^{1/2}(s-\mu_2 c)\}\right],$$

$$K_{22} = \mathrm{Re}\left[\frac{1}{\mu_2-\mu_1}\{(c+\mu_1 s)^{1/2}(s-\mu_1 c) - (c+\mu_2 s)^{1/2}(s-\mu_2 c)\}\right]. \tag{7a–d}$$

Note from (4) that the hoop and shear stresses in the vicinity of the crack tip take on the form

$$\sigma_{\omega\omega} = \frac{K_{\omega\omega}}{\sqrt{2\pi r}}, \quad \sigma_{r\omega} = \frac{K_{r\omega}}{\sqrt{2\pi r}}. \tag{8a,b}$$

These equations provide an explicit form for the stresses which exist normal to and along the kink line for the points in the vicinity of the crack tip, before the kink occurs. Displacements can also be calculated in the same way as stresses. They are

$$u_x = \sqrt{\frac{2r}{\pi}}[u_{11}K_{\mathrm{I}}^{\infty} + u_{12}K_{\mathrm{II}}^{\infty}], \quad u_y = \sqrt{\frac{2r}{\pi}}[u_{21}K_{\mathrm{I}}^{\infty} + u_{22}K_{\mathrm{II}}^{\infty}], \tag{9a,b}$$

where

$$u_{11} = \mathrm{Re}\left[\frac{1}{\mu_1 - \mu_2}\{\mu_1 p_2 (c+\mu_2 s)^{1/2} - \mu_2 p_1 (c+\mu_1 s)^{1/2}\}\right],$$

$$u_{12} = \mathrm{Re}\left[\frac{1}{\mu_1 - \mu_2}\{p_2 (c+\mu_2 s)^{1/2} - p_1 (c+\mu_1 s)^{1/2}\}\right],$$

$$u_{21} = \mathrm{Re}\left[\frac{1}{\mu_1 - \mu_2}\{\mu_1 q_2 (c+\mu_2 s)^{1/2} - \mu_2 q_1 (c+\mu_1 s)^{1/2}\}\right],$$

$$u_{22} = \mathrm{Re}\left[\frac{1}{\mu_1 - \mu_2}\{q_2 (c+\mu_2 s)^{1/2} - q_1 (c+\mu_1 s)^{1/2}\}\right], \tag{10a–d}$$

where $p_i = C_{11}\mu_i^2 - C_{16}\mu_i + C_{12}$ and $q_i = C_{12}\mu_i + C_{22}/\mu_i - C_{26}$.

Displacements in the rotated coordinate system then are

$$u_r \equiv u_x \cos\omega + u_y \sin\omega \quad \text{and} \quad u_\omega \equiv u_y \cos\omega - u_x \sin\omega. \tag{11a,b}$$

Energy-release rate for a collinear extension of the main crack

The energy-release rate can be computed following Irwin's method, as shown by Sih *et al.* (1965). Consider a closure of a crack segment by a distance δ, *collinear with the existing crack*. The required energy for this closure is the energy-release rate, G, given by the integral

$$G \equiv \lim_{\delta \to 0} \frac{1}{\delta} \int_0^{\delta} [\sigma_{yy}(r,0)\, u_y(\delta - r, \pi) + \sigma_{xy}(r,0)\, u_x(\delta - r, \pi)]\, \mathrm{d}r. \tag{12}$$

By substituting the appropriate expressions for the stress components from (8) and displacement components from (9) into (12), one obtains

$$G = \frac{1}{2} C_{11}\, \mathrm{Im}\left[-k_{\mathrm{I}}^2 \left(\frac{C_{22}}{C_{11}} \frac{\mu_1 + \mu_2}{\mu_1 \mu_2}\right) + k_{\mathrm{II}}^2 (\mu_1 + \mu_2) + k_{\mathrm{I}} k_{\mathrm{II}} \left(\mu_1 \mu_2 - \frac{C_{22}}{C_{11}} \frac{1}{\mu_1 \mu_2}\right)\right], \tag{13a}$$

where k_{I} and k_{II} are the commonly used modes I and II stress intensity factors at the crack tip. For an infinitely extended plane containing a central crack and loaded uniformly at infinity, one has $k_{\mathrm{I}} = K_{\mathrm{I}}^{\infty}$ and $k_{\mathrm{II}} = K_{\mathrm{II}}^{\infty}$. If the material is orthotropic and the body-coordinates coincide with the material-symmetry coordinates, i.e. when the crack is on one plane of material symmetry, then $C_{16} = C_{26} = 0$, and, under these conditions, (13a) reduces to

$$G = \frac{1}{2} C_{11} \operatorname{Im}[-k_{\mathrm{I}}^2(\mu_1+\mu_2)\overline{\mu_1}\,\overline{\mu_2} + k_{\mathrm{II}}^2(\mu_1+\mu_2) - 2k_{\mathrm{I}}k_{\mathrm{II}}(\overline{\mu_1}\,\overline{\mu_2})]. \tag{13b}$$

If the crack and its collinear extension are located at an arbitrary angle λ with respect to the material symmetry coordinates, then (13b) becomes

$$G = \frac{1}{2} C'_{11} \operatorname{Im}[-k_{\mathrm{I}}^2(\mu'_1+\mu'_2)\overline{\mu'_1}\,\overline{\mu'_2} + k_{\mathrm{II}}^2(\mu'_1+\mu'_2) - 2k_{\mathrm{I}}k_{\mathrm{II}}(\overline{\mu'_1}\,\overline{\mu'_2})], \tag{13c}$$

where μ'_i and C'_{11} are given by

$$\mu'_i = \frac{\mu_i \mathrm{c} - \mathrm{s}}{\mathrm{c} + \mu_i \mathrm{s}} \tag{14a}$$

and

$$C'_{11} = C_{11}\mathrm{c}^4 + (2C_{12}+C_{66})\mathrm{s}^2\mathrm{c}^2 + C_{22}\mathrm{s}^4 + 2\mathrm{sc}(C_{16}\mathrm{c}^2 + C_{26}\mathrm{s}^2). \tag{14b}$$

Here, s and c stand for sine and cosine of angle λ (λ is considered positive for anti-clockwise rotation from the material coordinate system to the crack direction; in Fig. 1, $\lambda = -\theta$).

Modified Irwin's formula

Equations (13a–c) express the energy-release rate when a crack (with no kink) tends to extend collinearly. It is a common practice to apply the expressions (13a–c), with suitable modification, to a kink of an arbitrary angle. This is justified as follows. Consider the crack kinking depicted in Fig. 1. Assume a kink of length L at angle ω at the right tip of the main crack of length $2a$. The singularity in the stress field around the kink tip is similar to that at the tip of a crack without a kink, and as a result, the asymptotic expressions for the stress and displacement fields in the vicinity of these tips are identical. This suggests that, for obtaining the energy-release rate for a non-collinear crack extension (kinking), it suffices to substitute the stress intensity factors $K_{\mathrm{I}}^{(\mathrm{k})}$ and $K_{\mathrm{II}}^{(\mathrm{k})}$ (calculated at the tip of a vanishingly small kink; calculation of $K_{\mathrm{I}}^{(\mathrm{k})}$ and $K_{\mathrm{II}}^{(\mathrm{k})}$ will be presented shortly) into (13c) to arrive at

$$G^{\mathrm{Irwin}} = \frac{C'_{11}}{2} \operatorname{Im}[-K_{\mathrm{I}}^{(\mathrm{k})}K_{\mathrm{I}}^{(\mathrm{k})}(\mu'_1+\mu'_2)\overline{\mu'_1}\,\overline{\mu'_2} + K_{\mathrm{II}}^{(\mathrm{k})}K_{\mathrm{II}}^{(\mathrm{k})}(\mu'_1+\mu'_2) - 2K_{\mathrm{I}}^{(\mathrm{k})}K_{\mathrm{II}}^{(\mathrm{k})}(\overline{\mu'_1}\,\overline{\mu'_2})]. \tag{15}$$

Note, again, that C'_{11}, μ'_1, and μ'_2 are defined in the ζ, η-coordinate system; see Fig. 1.

This modified result expresses the energy-release rate for an infinitesimal extension of an *existing* infinitesimally small kink, and may not give the energy that is released due to the *occurrence* of kinking (the *kink nucleation energy*). To obtain the kink nucleation energy, we must calculate the energy-release rate from its original definition (12). To do this, we need first to calculate the kink opening displacements (KODs); the components of KOD in the r- and ω-directions are u_{r} and u_{ω} in (11). Then, we

use the hoop stresses $\sigma_{\omega\omega}$ and $\sigma_{r\omega}$ in (12), and obtain the rate of energy released due to kink nucleation, G^{kink}, directly.

Kinked crack formulation

To solve the kinked-crack problem, a method similar to that of Lo (1978) is employed, where a continuous distribution of edge dislocations along the kink line is used to model the discontinuity across the kink surface. Obata *et al.* (1989) applied this method to solve the kink problem in an anisotropic solid. We use the formulation by Obata *et al.* (1989) to calculate the aforementioned distribution of edge dislocations along the kink line. Obara *et al.* (1989) show that the condition of stress-free kink surfaces results in a system of coupled, singular integral equations where the unknowns are the continuously distributed edge dislocations along the kink line, $b_x(s)$ and $b_y(s)$; with $b = b_x(s) + \mathrm{i}\, b_y(s)$.

The dislocation density functions $b_x(s)$ and $b_y(s)$ are singular at the kink knee and at the kink tip. One can extract the singularity from the dislocation density functions as follows

$$b_x(s) = \frac{B_x(s)}{\sqrt{s(L-s)}}, \quad (B_x(0) = 0) \quad \text{and} \quad b_y(s) = \frac{B_y(s)}{\sqrt{s(L-s)}}, \quad (B_y(0) = 0), \tag{16a,b}$$

where L is the kink length, s is measured along the kink line from the kink knee, and B_x and B_y are the non-singular parts of b_x and b_y that are assumed to be smooth functions (Figs 1 and 3). Note that the conditions given in (16), for $s = 0$, take into account the fact that the *singularity at the kink knee is less than one half*; see Bogy (1971) and Azhdari (1995). In view of (16), $B_x(s)$ and $B_y(s)$ are now the unknown functions which must be calculated.

In order to numerically solve the system of coupled singular integral equations, B_x and B_y are interpolated using N piecewise quadratic polynomials; see Gerasoulis (1982) (for $N > 100$, convergence to essentially the same values is obtained). Then, the singular parts of the integrals are integrated analytically, and the non-singular parts are obtained numerically. This leads to a system of $2(2N+1)$ algebraic linear equations. Once this system is solved, values of B_x and B_y at $2N+1$ distinct points along the kink line are known. Obata *et al.* (1989) show that

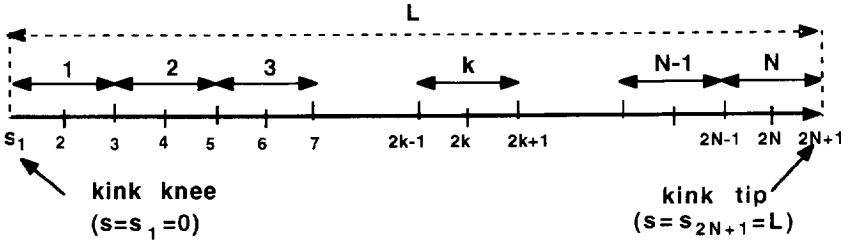

Fig. 3. Nodal discretization along the kink line for numerical routine.

$$K_{\mathrm{I}} = \pi\sqrt{\frac{2\pi}{L}}[M_{11}B_x(L)+M_{12}B_y(L)], \quad K_{\mathrm{II}} = \pi\sqrt{\frac{2\pi}{L}}[M_{21}B_x(L)+M_{22}B_y(L)], \tag{17a,b}$$

where M_{ij}s are some known functions of material properties and the kink angle ω. This summarizes the formulation of Obata *et al.* (1989).

For a vanishingly small kink, denote K_{I} and K_{II}, by $K_{\mathrm{I}}^{(\mathrm{k})}$ and $K_{\mathrm{II}}^{(\mathrm{k})}$, respectively (these stress intensity factors are used in the modified Irwin formula). For this case, in the numerical routine, the ratio of the kink length to the main crack length is chosen to be a very small number, e.g. $L/a < 10^{-6}$. An alternative way for handling the vanishingly small kink is to consider $L/a \ll 1$, and then show that B_x and B_y along the kink line are proportional to $\sqrt{L}$; see Azhdari (1995) and also Appendix. Thus, $K_{\mathrm{I}}^{(\mathrm{k})}$ and $K_{\mathrm{II}}^{(\mathrm{k})}$ become independent of length L, and as a result, the numerical routine becomes independent of the kink length.

Calculation of kink opening displacement (KOD)

Once $B_x(s)$ and $B_y(s)$ are calculated, then the dislocation density functions $b_x(s)$ and $b_y(s)$ are known from (16). The kink gap (kink opening displacements, KODs) can be derived from the dislocation density functions as follows

$$[u_x](s) = -\int_L^s b_x(\xi)\,\mathrm{d}\xi \quad \text{and} \quad [u_y](s) = -\int_L^s b_y(\xi)\,\mathrm{d}\xi, \tag{18a,b}$$

where [ ] denotes the jump of the corresponding argument (e.g. Nemat-Nasser and Hori, 1993). Here, we briefly explain the numerical routine used to perform the above integration. First, partition the kink length [0, L] into N subintervals; see Fig. 3. Within each subinterval, interpolate $B_x(s)$ and $B_y(s)$ by appropriate quadratic functions. Use these interpolation functions along with (16), and then carry out the integration in (18). The details for this numerical integration are given by Azhdari (1995). The above procedure gives the KODs in the x- and y-directions ($[u_x](s)$ and $[u_y](s)$) at all distinct points considered along the kink line. Then, the KODs in the kink and normal to the kink directions are obtained from

$$U \equiv [u_{\mathrm{r}}] \equiv [u_x]\cos\omega + [u_y]\sin\omega \quad \text{and} \quad V \equiv [u_\omega] \equiv [u_y]\cos\omega - [u_x]\sin\omega. \tag{19}$$

The KODs of $2N+1$ distinct points along the kink line are known. In order to calculate the KODs of all points along the kink line, one can interpolate these nodal KODs. We choose to use, again, quadratic polynomials to interpolate the nodal data. The kink opening displacements (KODs) of all the points along the kink line are then calculated. The stresses acting on this line (before kinking) are already known; see $\sigma_{\omega\omega}$ and $\sigma_{\mathrm{r}\omega}$ given in (8). Therefore, now, all ingredients are provided to calculate the energy-release rate at the inception of kinking.

Energy-release rate due to kink nucleation (G^{kink})

The work required for closure of the gap created by the nucleation of a kink is the energy that is released when crack kinking occurs. Before kinking, the state of stress

is the hoop and shear stresses given by (8), and also no gap existed along the potential kink line. After kinking, the hoop and shear stresses along the kink line are zero, but the kink opening displacements calculated by (19) are non-zero. In fact, physically, these two field quantities should be compatible, i.e. the stresses ($\sigma_{\omega\omega}$ and $\sigma_{r\omega}$) and displacements (V and U) are related by (2). Mathematically, the energy (per unit kink length) required to fully close the kink gap is

$$G^{\text{kink}} \equiv \frac{1}{2}\lim_{L\to 0}\frac{1}{L}\int_0^L \{\sigma_{\omega\omega}(r,\omega)\,[u_\omega]+\sigma_{r\omega}(r,\omega)\,[u_r]\}\,\mathrm{d}r. \tag{20}$$

Substituting for the stresses from (8) and for the KODs from (19), one arrives at

$$G^{\text{kink}} = \frac{1}{2}\lim_{L\to 0}\frac{1}{L}\int_0^L\left[\frac{K_{\omega\omega}}{\sqrt{2\pi r}}V+\frac{K_{r\omega}}{\sqrt{2\pi r}}U\right]\mathrm{d}r. \tag{21}$$

Now, change the variable r as $r = L(1+\hat{s})/2$ and also partition the interval $[0, L]$ into N sub-intervals; see Fig. 3. This changes (21) to

$$G^{\text{kink}} = \frac{1}{2\sqrt{2\pi}}\lim_{L\to 0}\frac{1}{L}\sum_{k=1}^{k=N}\int_{\hat{s}_{2k-1}}^{\hat{s}_{2k-1}}[K_{\omega\omega}\,V^{(k)}(\hat{s})+K_{r\omega}\,U^{(k)}(\hat{s})]\frac{L/2}{\sqrt{L(\hat{s}+1)/2}}\mathrm{d}\hat{s}. \tag{22}$$

Azhdari (1995) has shown that, when the kink length is vanishingly small, then the dislocation density functions, $B_x(s)$ and $B_y(s)$, are proportional to $\sqrt{L}$ (this is briefly demonstrated in the Appendix). As a result, considering (18), the KODs (V and U) are also proportional to $\sqrt{L}$, and therefore, this cancels out all Ls in (22). Considering this fact, the energy-release rate is independent of the vanishingly small length of the kink, and therefore, the procedure for taking the "limit" in (20) becomes immaterial. This changes (22) to

$$G_{\text{kink}} = \frac{1}{4\sqrt{\pi}}\sum_{k=1}^{k=N}\int_{\hat{s}_{2k-1}}^{\hat{s}_{2k+1}}[K_{\omega\omega}\,V^{(k)}(\hat{s})+K_{r\omega}\,U^{(k)}(\hat{s})]\frac{1}{\sqrt{\hat{s}+1}}\mathrm{d}\hat{s}. \tag{23}$$

In terms of V and U from (19), the integrand in (23) is fully defined and the integration can easily be performed. For details, see Azhdari (1995).

This equation gives the energy-release rate due to the nucleation of an infinitesimally small kink at the angle ω. The numerical results of this equation will be compared with the results from the commonly used energy-release-rate formula, namely the modified Irwin formula, G^{Irwin} (15).

RESULTS

The main objective of this work is to investigate whether the Irwin formula gives the energy that is released during the process of kink nucleation. Once this is established, we then compare the energy-release-rate fracture criterion with other criteria for anisotropic solids.

Numerical calculations are performed for the special case of orthotropic materials,

where $C_{16} = C_{26} = 0$; this eases the calculation of the roots of the characteristic equation (3), i.e.

$$\hat{C}_{11}\hat{\mu}^4 + (2\hat{C}_{12} + \hat{C}_{66})\hat{\mu}^2 + \hat{C}_{22} = 0, \tag{24}$$

where the symbols with hats are the equivalent symbols for C_{11}, C_{22}, C_{12}, C_{66}, and μ; see the x_1, x_2- and x, y-coordinate systems in Fig. 1. The on-axis orthotropic constants can be written in terms of Young's moduli, the shear modulus, and Poisson's ratios as

$$\hat{C}_{11} = \frac{1}{E_{11}}, \quad \hat{C}_{22} = \frac{1}{E_{22}}, \quad \hat{C}_{66} = \frac{1}{E_{66}}, \quad \hat{C}_{12} = -\frac{\nu_1}{E_{11}} = -\frac{\nu_2}{E_{22}}. \tag{25}$$

The stress intensity factors and the energy-release rate are non-dimensionalized so that HSIF and G take on the value of "one" at $\omega = 0$. Setting $\omega = 0$ in (5a) and (13), gives the required terms for non-dimensionalization

$$K_0 \equiv K_{\omega\omega}(\omega = 0) = K_{\mathrm{I}}^{(\mathrm{k})}(\omega = 0) = K_{\mathrm{I}}^{\infty} = \sigma_{yy}^{\infty}\sqrt{\pi a}, \quad G_0 \equiv G(\omega = 0). \tag{26a,b}$$

If σ_{yy}^{∞} is zero, we replace σ_{yy}^{∞} by σ_{xy}^{∞} in (26a). Note that G_0 is the energy-release rate for collinear extension of the main crack. Therefore, $r_G = G^{\mathrm{Irwin}}/G_0 = 1$ (or $r_G = G^{\mathrm{kink}}/G_0 = 1$) is associated with collinear crack extension.

Validity of Irwin's formula for G calculation

This investigation can be performed numerically, because the required quantities to calculate G^{Irwin} ($K_{\mathrm{I}}^{(\mathrm{k})}$ and $K_{\mathrm{II}}^{(\mathrm{k})}$) and G^{kink} (KODs) can only be calculated numerically. The results depend not only upon the value of the kink angle, but also on other parameters, e.g. the material properties (for example, E_{11} and E_{22}), material symmetry orientation θ, and the applied stresses σ_{yy}^{∞} and σ_{xy}^{∞}. Of course, consideration of all possible combinations of all the involved parameters is very difficult. Therefore, we examine only a few extreme examples, as summarized in Table 1.

The correlation between G^{Irwin} and G^{kink} is examined at kink angles where $K_{\mathrm{I}}^{(\mathrm{k})}$ (lines 1, 3, 5, and 6 of Table 1), $K_{\omega\omega}$ (lines 3 and 8 of Table 1), and G^{kink} (line 9 of Table 1) are maximum. As is seen from Table 1, the energy-release rate calculated by using both modified Irwin (G^{Irwin}) and the direct (G^{kink}) methods is the same. Therefore, Irwin's formula for the energy-release rate is valid for any kink angle, material anisotropy, and loading condition (any combination of modes I and II), provided that the stress intensity factors in the formula are taken equal to those calculated at the tip of a vanishingly small kink, and all other involved parameters are transferred from the crack to the kink direction. It is thus established that the modified Irwin formula yields the energy-release rate due to kink nucleation, as well as kink extension; see also the Appendix where this fact is further discussed based on semi-analytical results.

Table 1. *Comparison of* G^{Irwin} *and* G^{kink} *under different conditions* ($\nu_2 = 0.25$, $N = 200$)

E_{11}	E_{22}	E_{66}	β	ω	σ_{yy}^{∞}	σ_{xy}^{∞}	$K_{\text{I}}^{(k)}/K_0$	$K_{\omega\omega}/K_0$	$K_{\text{II}}^{(k)}/K_0$	$K_{r\omega}/K_0$	G^{Irwin}/G_0	G^{kink}/G_0
1	1	0.4	0°	−77°	0	100	1.2289*	1.1438	0.0038	0.1272	1.5104	1.5103
8	1	0.8	60°	−150°	32	48	0.4925	0.1886	−0.3091	−0.5005	0.2163	0.2163
8	1	0.8	60°	−55°	32	48	2.3039*	2.2896*	0.0104	−0.0248	1.6017	1.6016
8	1	0.8	60°	−90°	32	48	1.7853	1.7193	−0.9834	−1.0885	1.4007	1.4006
9	1	1.38	2°	−49°	100	2	1.1321*	1.1222	−0.0147	−0.0252	0.7791	0.7791
1	10	0.4	45°	−89°	0	100	1.0360*	0.7419	0.0526	−0.2979	1.0388	1.0381
1	4	0.4	30°	−90°	0	100	1.0820	0.9056	−0.0987	−0.3549	1.2306	1.2306
1	10	0.4	45°	−61°	0	100	0.9316	0.8577*	0.2161	−0.0008	1.1656	1.1656
2	10	0.4	30°	36.3°	100	20	1.0095	1.0074	−0.1601	−0.1684	1.2242*	1.2242*
1	2	0.4	−30°	−90°	100	0	0.2403	0.2389	−0.3901	−0.3786	0.1903	0.1903
2	10	0.4	30°	−90°	100	20	0.7379	0.6437	−0.2215	−0.3575	0.8053	0.8053
8	1	0.8	−45°	45°	100	50	0.0962	0.1035	0.8870	0.8651	0.6757	0.6757
1	20	0.8	−60°	45°	50	−50	1.7103	1.6003	−0.5620	−0.1911	1.3116	1.3116

* The corresponding quantity (shown in the top row) is maximum at the relevant kink angle.

Comparison of different fracture criteria under general loading

Next, compare different fracture criteria for the case of asymmetric loading (general loading, shear or shear along with tension). This problem has not been extensively examined by previous investigators (especially for the case of pure shear); see Obata *et al.* (1989) and Gao and Chiu (1992). Moreover, owing to two factors, we re-examine the problem here. These factors are: (1) all tools (numerical routines) for calculating different quantities are ready, and (2) we can assess the viability of the maximum HSIF fracture criterion (which is a form of the maximum hoop stress fracture criterion) in comparison with other fracture criteria, for anisotropic solids.

It is well established that, in isotropic materials, the commonly used fracture criteria, i.e. (1) maximum-K_I; (2) zero-K_{II}; (3) maximum-hoop stress; and (4) maximum energy-release rate, lead to similar fracture predictions (to the first order in the kink angle). The greatest dissimilarity among the predictions of these fracture criteria occurs when the loading is a pure shear one (the most asymmetric case for isotropic materials); the corresponding equations show that the crack would kink at angles of about $-71°$, $-75°$, and $-77°$, according to fracture criteria maximum-HSIF, maximum-K_I (or zero-K_{II}), and maximum energy-release rate, respectively. As is seen, these fracture criteria are fairly consistent in predicting the kink path (the consistency is better when the loading is less asymmetric, i.e. some tensile load is also applied).

In contrast, in the case of general anisotropy, asymmetry can be created by different sources, e.g. material properties, material orientation, applied loads, and the overall geometry of the specimen. In addition, the material resistance to fracturing, in general, is orientation dependent and anisotropic, especially in single crystals. For simplicity, here, *we assume that fracture resistance is uniform throughout the body* which is *not* true for actual anisotropic solids. The combination of the asymmetries generated by these sources makes the crack kinking process very complicated and therefore observation of a consistent prediction by different fracture criteria for anisotropic materials is not expected.

The following seven different sets of conditions are considered for a general loading, to reveal the variation of HSIF (which is based on the field quantities prior to crack kinking), $K_I^{(k)}$, and the energy-release rate (which is based on the field quantities after crack kinking), with respect to the kink angle ω; for more examples see Azhdari (1995). These sets are:

Case (1) $\alpha = 0.0$, $\theta = 0°$, Fig. 4; Case (2) $\alpha = 0.0$, $\theta = 5°$, Fig. 5;
Case (3) $\alpha = 0.1$, $\theta = 5°$, Fig. 6; Case (4) $\alpha = 0.3$, $\theta = 30°$, Fig. 7;
Case (5) $\alpha = 1.0$, $\theta = 45°$, Fig. 8; Case (6) $\alpha = \infty$, $\theta = 0°$, Fig. 9;
Case (7) $\alpha = \infty$, $\theta = 30°$, Fig. 10;

where $\alpha = K_{II}^{\infty}/K_I^{\infty} = \sigma_{xy}^{\infty}/\sigma_{yy}^{\infty}$; see (6). In all cases, $E_{66} = 0.4$ and $\nu_2 = 0.25$. Moreover, in each figure, the corresponding values of the anisotropy ratio E_{11}/E_{22} (or E_{22}/E_{11}) are explicitly given. The following observations are the results of these computational investigations:

(a) Unlike the isotropic case, for anisotropic solids, the K-based and G-based fracture criteria, in general, do not predict the same angle for crack kinking. As

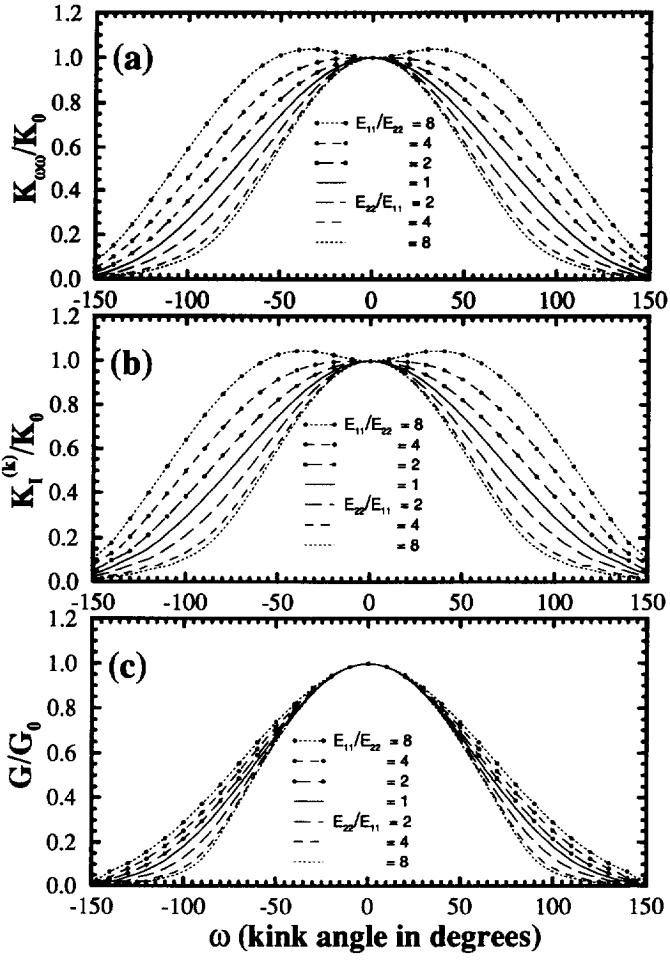

Fig. 4. Variation of (a) HSIF, (b) mode-I SIF, and (c) G versus ω for $\theta = 0^\circ$, $\alpha = 0.0$ (pure tensile stress).

observed from Figs 4–10, the trend of the G- and SIF-curves are similar for $E_{22}/E_{11} \geqslant 1$, but are different for $E_{11}/E_{22} > 1$. This difference is more pronounced when the loading is pure shear; see Figs 9 and 10. Hence, in general, the energy-release-rate fracture criterion does not appear to predict a crack propagation path similar to the ones predicated by other stress-based fracture criteria.

(b) As observed from all the cases, the trends of the HSIF- and $K_I^{(k)}$-curves are always similar. In particular, it is observed that in general, when the kink angle is between -8° and $+8^\circ$, then the difference between HSIF and $K_I^{(k)}$ is less than 1.0%; see Azhdari and Nemat-Nasser (1995). This range (-8° to $+8^\circ$) widens as E_{11} approaches E_{22}, and narrows for very large or very small ratios of E_{11}/E_{22}. In general, the larger the kink angle, the larger the difference between the values of HSIF and $K_I^{(k)}$; for certain cases, these quantities can differ by a factor of two or more. There are also many cases for which this difference is very small (around 1%), even for kink

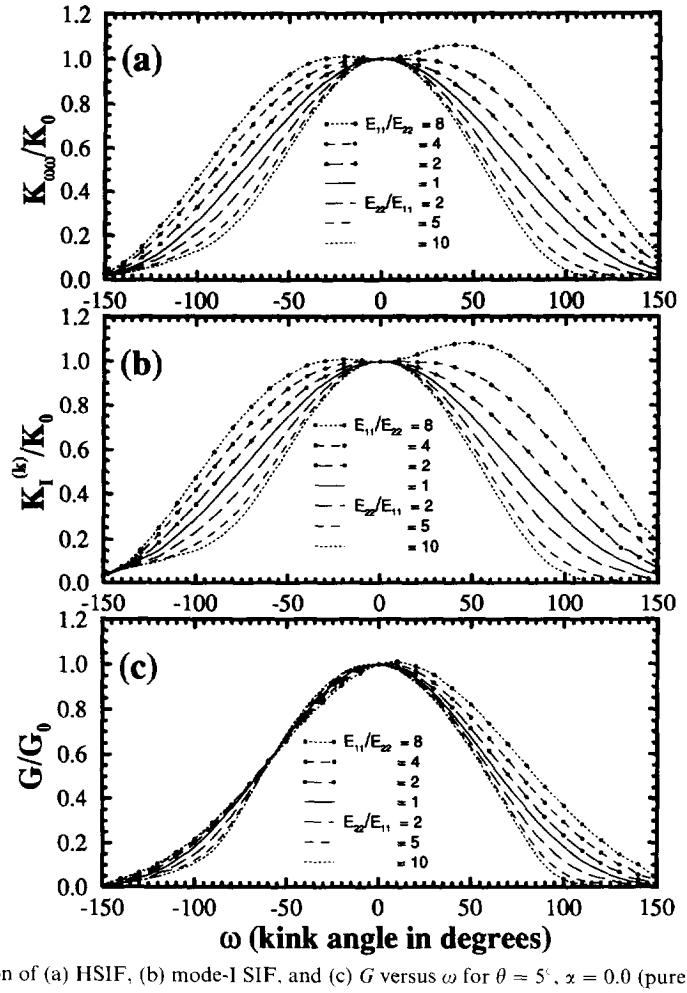

Fig. 5. Variation of (a) HSIF, (b) mode-I SIF, and (c) G versus ω for $\theta = 5^\circ$, $\alpha = 0.0$ (pure tensile stress).

angles as large as 100°. For many of the cases examined, it is observed that the kink angles which render HSIF and $K_I^{(k)}$ maximum are close to each other, even when the magnitudes of these two quantities are quite different.

(c) For small values of the anisotropy ratio $r^{(12)} = E_{11}/E_{22}$, the HSIF and $K_I^{(k)}$ have only one maximum point; see, e.g. Figs 4(a) and (b), 5(a) and (b). However, as materials with larger anisotropy ratio than a critical ratio $r_c^{(12)}$ are considered, it is observed that the HSIF- and $K_I^{(k)}$-curves display two maxima with a local minimum in between. For example, Fig. 4(a) shows that the HSIF has an absolute maximum for $r^{(12)} < r_c^{(12)} = 4$, one local minimum, and two symmetrically located maxima (with respect to $\omega = 0$) for $r^{(12)} > 4$ (similar behavior is observed from Fig. 4(b) for $K_I^{(k)}$). Figure 5(a) and (b) shows yet other examples where the two maxima are not located symmetrically with respect to $\omega = 0$, and these show that the corresponding $r_c^{(12)}$ is slightly less than four. Similarly, in Fig. 6(a) and (b), the local minimum occurs for

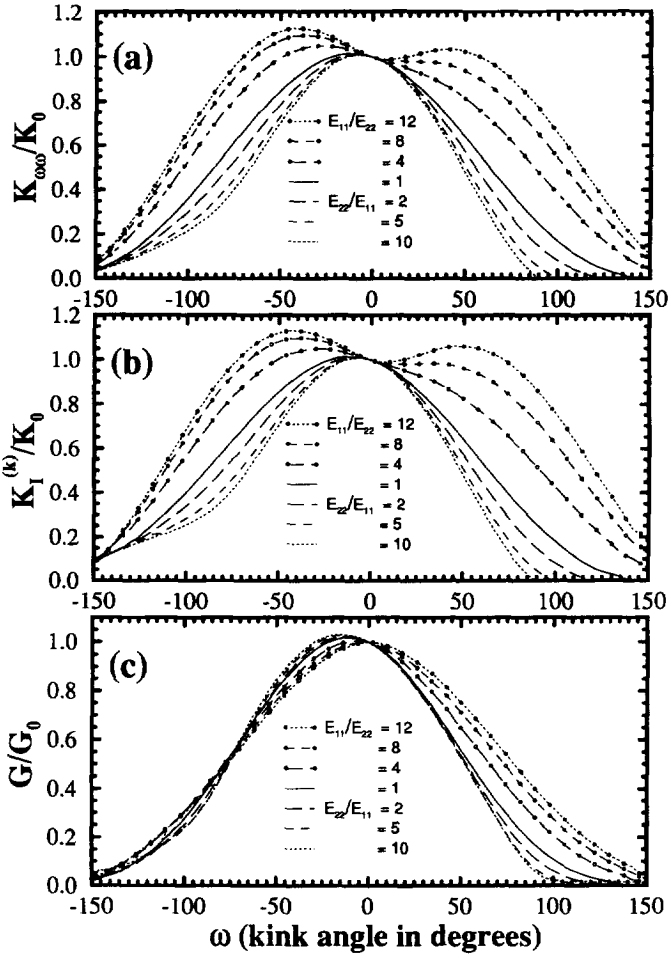

Fig. 6. Variation of (a) HSIF, (b) mode-I SIF, and (c) G versus ω for $\theta = 5$, $\alpha = 0.1$.

$r^{(12)}$ between 4 and 8 ($r_c^{(12)} \approx 7$). For stiffness ratios greater than these values, the HSIF-curves possess two maxima with a minimum in between. Moreover, it is observed that as materials with relatively larger ratios than $r_c^{(12)}$ are considered, the corresponding location of the absolute maximum of the associated HSIF- and $K_I^{(k)}$-curves may shift from one side of the local minimum point to the other. In other words, for a certain value of the stiffness ratio, the angle at which the HSIF and/or $K_I^{(k)}$ become maximum may have a jump.

(d) The G-curve may also display a similar variation with respect to changes in $r^{(12)}$, as discussed in section (c) for the SIFs; see the G-curves in Figs 9(c) and 10(c), where the curves possess two maxima and one local minimum point in between (note that these curves correspond to pure shear, $\alpha = \infty$). Now, consider the fact that cracks generally propagate into tension (but not compression) zones; therefore, the interpretation of the fracture mode and the branch angle must be accompanied by

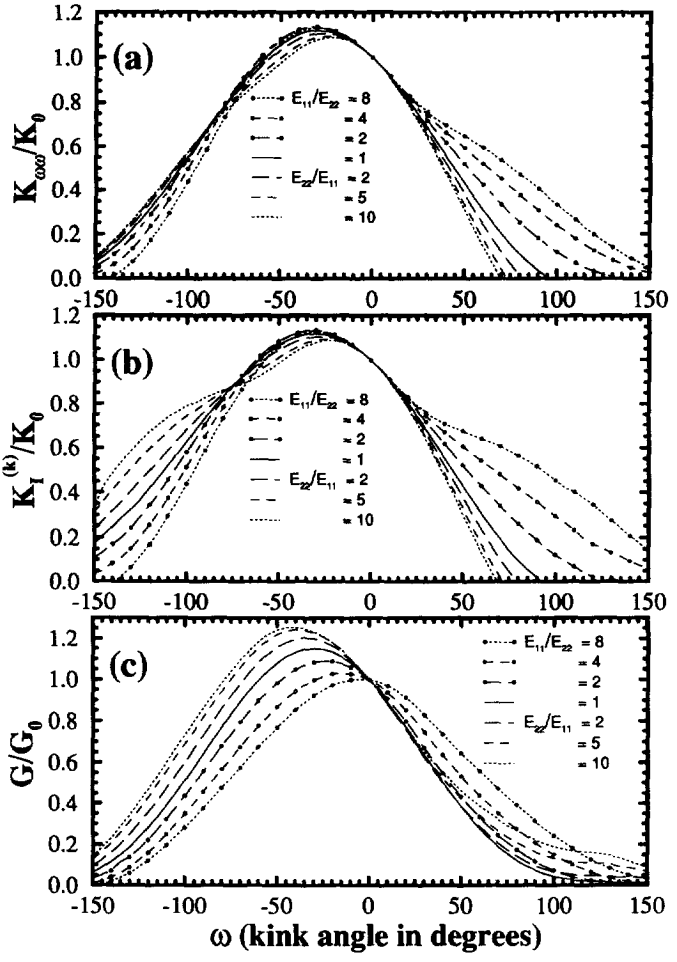

Fig. 7. Variation of (a) HSIF, (b) mode-I SIF, and (c) G versus ω for $\theta = 30^\circ$, $\alpha = 0.3$.

the consideration of the HSIF at the maxima of the G-curve. For example, consider Fig. 9(c), where the G-curve has a local minimum and two equal maxima, symmetrically located with respect to $\omega = 0^\circ$. Here, HSIF is positive when ω is negative and therefore, fracture may occur only for negative ω. Another example is the case depicted in Fig. 10(c) where θ is non-zero and therefore, the G-curves are not symmetric with respect to $\omega = 0^\circ$. It is possible to find cases where the absolute maximum of the G-curve happens at an angle, where HSIF is negative, and therefore, the other maximum of the G-curve has to be considered for the fracture prediction. This indicates that the G-fracture criterion (by itself) is not sufficient for describing the phenomenon of kinking.

(e) Next, let us look at the possibility of kinking and/or branching (forking) of the main crack. Crack branching may occur when the fracture criterion offers almost equal opportunity (energy for the G-criterion and stress for SIF-criteria) for the crack

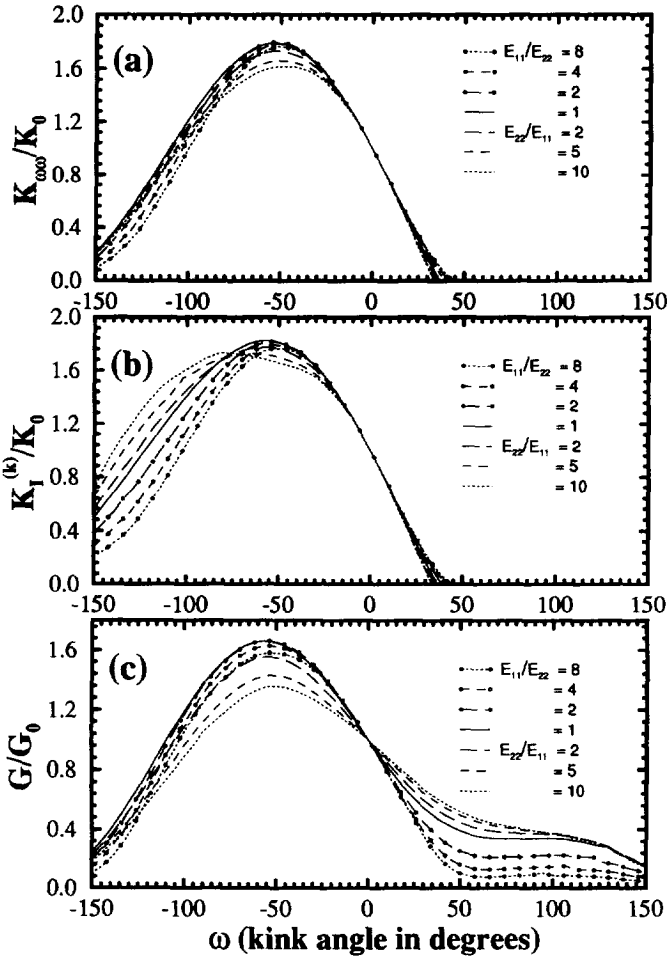

Fig. 8. Variation of (a) HSIF, (b) mode-I SIF, and (c) G versus ω for $\theta = 45^\circ$, $\alpha = 1.0$.

to open in two or more directions. Figure 4(a) and (b) suggests that for $E_{11}/E_{22} = 8$, the main crack should branch in two directions of $\omega \approx 35^\circ$ and $\omega \approx -35^\circ$, where the SIF (either HSIF or $K_I^{(k)}$) is maximum. In contrast, Fig. 4(c) shows that G is maximum at $\omega = 0^\circ$, and therefore, according to the G-criterion, the crack would not branch but kink at $\omega = 0^\circ$ (simply extends). This observation may serve to show how differently the G- and SIF-criteria may predict the fracture path. Note that here, again, we are not considering the effect of the material resistance to fracturing which should be considered in the prediction of the crack path.

The above observations raise the question of which fracture criterion is suitable for prediction of the fracture path in anisotropic solids. Only experiments may answer this question. In addition, the orientation dependence of the fracture resistance of the material (fracture resistance is also an anisotropic quantity in most anisotropic solids,

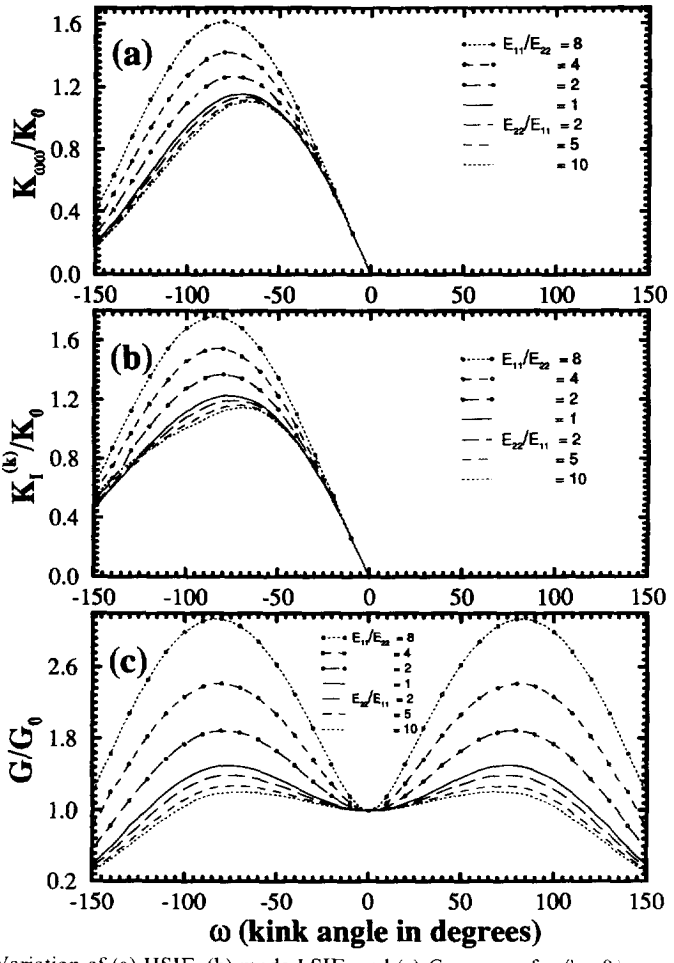

Fig. 9. Variation of (a) HSIF, (b) mode-I SIF, and (c) G versus ω for $\theta = 0^\circ$, pure shear.

especially in single crystals) makes the study of crack kinking more complex. Indeed, fracture anisotropy is usually larger than elastic anisotropy so that the direction of the crack will mainly be determined by crystallographic directions of the solid. In a work in process, this matter is somewhat challenged.

ACKNOWLEDGEMENTS

This work has been supported in part by ARO under Grant No. DAAL03-92-K-0002, and in part by the Institute for Mechanics and Materials (IMM), at the University of California, San Diego. Most of the computations reported here were carried out on a CRAY-YMP at the San Diego Supercomputer Center.

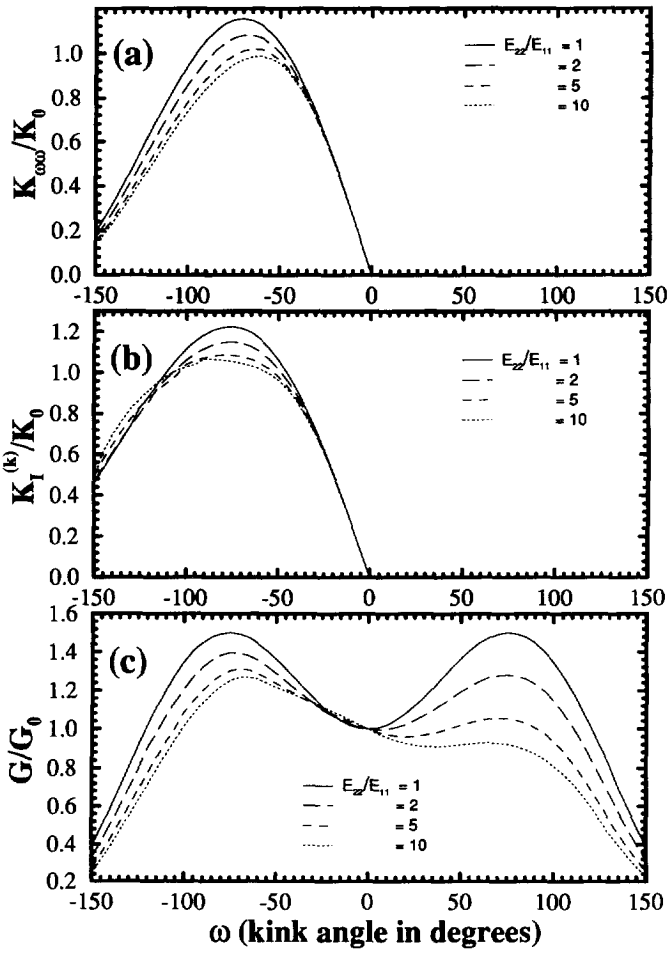

Fig. 10. Variation of (a) HSIF, (b) mode-I SIF, and (c) G versus ω for $\theta = 30^\circ$, pure shear.

REFERENCES

Azhdari, A. (1995) Fracturing in anisotropic brittle solids. Ph.D. Dissertation, University of California, San Diego.

Azhdari, A. and Nemat-Nasser, S. (1995) Hoop stress intensity factor and crack kinking in anisotropic brittle solids. *Int. J. Solids Structures* (in press).

Barnett, D. M. and Asaro, R. J. (1972) The fracture mechanics of slit-like cracks in anisotropic elastic media. *J. Mech. Phys. Solids* **20,** 353–366.

Bilby, B. A. and Eshelby, J. D. (1968) *Fracture, An Advanced Treatise Vol.* 1. *Microscopic and Macroscopic Fundamentals* (edited by H. Liebowitz), pp. 99–182.

Bogy, D. B. (1971) Two edge-bonded elastic wedges of different materials and wedge angles under surface tractions. *ASME J. Appl. Mech.* **38,** 377–386.

Gao, H. and Chiu, C. (1992) Slightly curved or kinked cracks in anisotropic elastic solids. *Int. J. Solids Structures* **29,** 947–972.

Gerasoulis, A. (1982) The use of piecewise quadratic polynomials for the solution of singular integral equations of Cauchy type. *Computers and Mathematics with Applications* **8,** 15–22.

Griffith, A. A. (1921) The phenomenon of rupture and flow in solids. *Phil. Trans. R. Soc.* **A221,** 163–198.
Griffith, A. A. (1924) The theory of rupture. *Proc. 1st Int. Congr. Appl. Mech.*, Delft, 55–63.
Gupta, G. D. (1976) Strain-energy-release rate for mixed crack problem. *ASME* 76-WA/PVP-7.
Hayashi, K. and Nemat-Nasser, S. (1981a) Energy release rate and crack kinking under combined loading. *ASME J. Appl. Mech.* **48,** 520–524.
Hayashi, K. and Nemat-Nasser, S. (1981b) Energy release rate and crack kinking. *Int. J. Solids Structures* **17,** 107–114.
Hussain, M. A., Pu, S. L. and Underwood, J. (1974) Strain-energy-release rate for a crack under combined Mode I and Mode II. *ASTM-STP*-560, 2–28.
Lekhnitskii, S. G. (1963) *Theory of Elasticity of an Anisotropic Elastic Body*. Holden-Day, San Francisco.
Lo, K. K. (1978) Analysis of branched cracks. *J. Appl. Mech.* **45,** 797–802.
Nemat-Nasser, S. (1979) The second law of thermodynamics and non-collinear crack growth. *Proceedings to Third Engineering Mechanics, Division Specialty Conference*, EMD of ASCE, The University of Texas at Austin, 17–19 September, pp. 449–452.
Nemat-Nasser, S. and Hori, M. (1993) *Micromechanics: Overall Properties of Heterogeneous Materials*. North Holland.
Obata, M., Nemat-Nasser, S. and Goto, Y. (1989) Branched cracks in anisotropic elastic solids. *J. Appl. Mech.* **56,** 858–864.
Palaniswamy, K. and Knauss, W. G. (1978) On the problem of crack extension in brittle solids under general loading. *Mechanics Today* (ed. S. Nemat-Nasser), pp. 87–148. Pergamon Press, Oxford.
Savin, G. N. (1961) *Stress Concentrations Around Holes*. Pergamon Press, Oxford.
Sih, G. C., Paris, P. C. and Irwin, G. R. (1965) On cracks in rectilinearly anisotropic bodies. *Int. J. Fracture Mech.* **1,** 189–203.
Sih, G. C. (1972) A special theory of crack propagation. *Mechanics of Fracture 1*. Noordhoff, Leyden.
Wu, C. H. (1978a) Elasticity problems of slender Z-crack. *J. Elasticity* **8,** 183–205.
Wu, C. H. (1978b) Maximum energy-release-rate criterion applied to a tension–compression specimen with crack. *J. Elasticity* **8,** 235–257.
Wu, C. H. (1979a) Fracture under combined loads by maximum-energy-release rate criterion. *J. Appl. Mech.* **46,** 553–558.
Wu, C. H. (1979b) Explicit asymptotic solution for the maximum energy-release-rate problem. *Int. J. Solids Structures* **15,** 561–566.

APPENDIX

For an infinitesimally small kink, Azhdari (1995) shows that the integral equations derived by Obata *et al.* (1989) can be simplified, leading to some interesting conclusions. Here, a summary is presented. Obata *et al.* (1989) show that the condition of stress-free kink surfaces results in a system of coupled, singular integral equations where the unknowns are the continuously distributed edge dislocations along the kink line, $b_x(s)$ and $b_y(s)$; with $\mathbf{b} = b_x(s) + \mathrm{i}\, b_y(s)$. The equations are as follows

$$\int_0^L \frac{M_{11} b_x(s) + M_{12} b_y(s)}{t-s}\,\mathrm{d}s + \int_0^L [L_{11}(s,t) b_x(s) + L_{12}(s,t) b_y(s)]\,\mathrm{d}s = -\sigma_{\theta\theta 0}(t),$$

$$\int_0^L \frac{M_{21} b_x(s) + M_{22} b_y(s)}{t-s}\,\mathrm{d}s + \int_0^L [L_{21}(s,t) b_x(s) + L_{22}(s,t) b_y(s)]\,\mathrm{d}s = -\sigma_{r\theta 0}(t), \quad 0 < t < L, \tag{A.1a,b}$$

where $\sigma_{\omega\omega}$ and $\sigma_{r\omega}$ are the hoop and shear stresses acting normal and along the kink line (before kinking), M_{ij}s are known functions of the material properties and the kink angle, and L_{ij}s are known functions of the material properties, kink angle, and X_{ij}s which are defined as

$$X_{ij}(z_i,z_j^0)=\frac{1}{z_i-z_j^0}\left[\frac{\sqrt{z_j^{0^2}-a^2}}{\sqrt{z_i^2-a^2}}-1\right],\quad i,j=1,2,3,4, \tag{A.2}$$

where for the points located on the kink line zs take on the following form

$$z_i=a+tH_i \quad \text{and} \quad z_j^0=a+sH_j, \quad \text{where} \quad H_{i,j}=\cos\omega+\mu_{i,j}\sin\omega. \tag{A.3a,b}$$

(μ_3 and μ_4 are complex conjugates of μ_1 and μ_2, respectively).

For a vanishingly small kink, Obata *et al.* (1989) assign a small number to L/a and then solve (A.1) numerically. Here, first, we simplify the aforementioned system of integral equations for the case of an infinitesimally small kink ($(L/a)^2\approx 0$) and then apply the appropriate numerical routine to solve the resulting system of integral equations.

To illustrate the approach, rewrite, for instance, (A.1a) as

$$\int_0^L \frac{M_{11}b_x(s)+M_{12}b_y(s)}{t-s}\,\mathrm{d}s+\int_0^L [N_x X_{ij}(s,t)\,b_x(s)+N_y X_{mn}(s,t)\,b_y(s)]\,\mathrm{d}s=-\sigma_{\omega\omega}(t), \tag{A.4}$$

where N_x and N_y are functions of the material properties and the kink angle only. Then, use (A.3) in (A.2) and obtain

$$X_{ij}(s,t)=\frac{1}{tH_i-sH_i}\left[\frac{\sqrt{sH_j(sH_j+2a)}}{\sqrt{tH_i(tH_i+2a)}}-1\right]. \tag{A.5}$$

Now, change the coordinates from (0 to L) to (0 to 1) using $\tilde{t}=t/L$ and $\tilde{s}=s/L$ and rewrite (A.5) as

$$X_{ij}(\tilde{s},\tilde{t})=\frac{1}{L(\tilde{t}H_i-\tilde{s}H_j)}\left[\frac{\sqrt{\dfrac{L^2}{a^2}\tilde{s}^2H_j^2+2\dfrac{L}{a}\tilde{s}H_j}}{\sqrt{\dfrac{L^2}{a^2}\tilde{t}^2H_i^2+2\dfrac{L}{a}\tilde{t}H_i}}-1\right]. \tag{A.6}$$

For small "L/a", set $(L/a)^2=0$ and obtain from (A.6)

$$X_{ij}(\tilde{s},\tilde{t})=\frac{1}{L(\tilde{t}H_i-\tilde{s}H_j)}\left[\frac{\sqrt{\tilde{s}H_j}}{\sqrt{\tilde{t}H_i}}-1\right]=\frac{-1}{L[\tilde{t}H_i+\sqrt{\tilde{t}\tilde{s}H_iH_j}]}=\frac{-1}{tH_i+\sqrt{tsH_iH_j}}. \tag{A.7}$$

Moreover, when the kink length is very small, the input function $\sigma_{\omega\omega}$ (or $\sigma_{r\omega}$) in (A.1) can be replaced by its asymptotic form given in (8) as

$$\sigma_{\omega\omega}(t)=\frac{K_{\omega\omega}}{\sqrt{2\pi t}}\Rightarrow\sigma_{\omega\omega}(\tilde{t})=\frac{K_{\omega\omega}}{\sqrt{2\pi L\tilde{t}}},\quad 0<t\leqslant L \quad \text{and} \quad 0<\tilde{t}\leqslant 1. \tag{A.8}$$

Now, use (A.7), (A.8), and (16) in (A.4) to arrive at

$$\frac{1}{L}\int_0^1 \frac{M_{11}B_x(\tilde{s})+M_{12}B_y(\tilde{s})}{(\tilde{t}-\tilde{s})\sqrt{\tilde{s}(1-\tilde{s})}}\,d\tilde{s}-$$

$$\frac{1}{L}\int_0^1 \left\{\frac{N_x B_x(\tilde{s})}{\tilde{t}H_i+\sqrt{\tilde{t}\tilde{s}H_iH_j}}+\frac{N_y B_y(\tilde{s})}{\tilde{t}H_m+\sqrt{\tilde{t}\tilde{s}H_mH_n}}\right\}\frac{1}{\sqrt{\tilde{s}(1-\tilde{s})}}\,d\tilde{s}=\frac{-K_{\omega\omega}}{\sqrt{2\pi L\tilde{t}}}. \quad \text{(A.9)}$$

Note that a similar equation is obtained, starting from (A.1b). Equation (A.9) explicitly shows the dependence of various terms on the vanishingly small kink length L.

From (A.9), the following conclusions can be drawn:

(1) Integrals of the (A.9) type are unavoidable even for the "vanishingly small L".
(2) The dislocation density functions, $B_x(s)$ and $B_y(s)$, are proportional to $\sqrt{L}$ for the "vanishingly small L".
(3) The stress intensity factors at the tip of a vanishingly small kink are independent of the "vanishingly small L"; see (17a,b).
(4) In view of conclusion (3) it is natural to expect that G^{Irwin} and G^{kink} should be the same, as is established numerically in this paper.